



Journal of Applied and Computational Mechanics



Research Paper

On Robust Adaptive PD Control of Robot Manipulators

Hancheol Cho 

Assistant Professor, Department of Mechanical Engineering, Bradley University, 1501 W Bradley Ave, Peoria, IL 61625, USA

Received November 07 2020; Revised December 03 2020; Accepted for publication December 03 2020.

Corresponding author: Hancheol Cho (hcho@fsmail.bradley.edu)

© 2020 Published by Shahid Chamran University of Ahvaz

Abstract. In this study, an adaptive proportional-derivative (PD) control scheme is proposed for trajectory tracking of multi-degree-of-freedom robot manipulators in the presence of model uncertainties and external disturbances whose upper bounds are unknown but bounded. The developed controller takes the advantages of linear control in the sense of simplicity and easy design, but simultaneously possesses high robustness against model uncertainties and disturbances while avoiding the necessity of precise knowledge of the system dynamics. Due to the linear feature of the proposed method, both the transient and steady-state responses are easily controlled to meet desired specifications. Also, an adaptive law for control gains using only position and velocity measurements is introduced so that parameter uncertainties and disturbances are successfully compensated, where the prior knowledge about their upper bounds is not required. Stability analysis is conducted using the Lyapunov's direct method and brief guidelines on how to select control parameters are also provided. Simulation results corroborate that the adaptive PD control law proposed in this paper can achieve a fast convergence rate, small tracking errors, low control effort, and small computational cost and its performance is compared with that of an existing nonlinear sliding mode control method.

Keywords: Adaptive control, PD control, Robot manipulator, Stability, Uncertainty.

1. Introduction

For the last few decades, the development of robust control schemes for robot manipulators has gained extensive interest due to its importance and practicality. Robust control strategies are designed to have good dynamic behavior, even when confronted with model uncertainties and external disturbances such as time-varying friction, backlash, and payload variation. Various control approaches have been proposed to achieve this goal, including feedback linearization [1-3], backstepping control [4-6], H_∞ control [7-9], passivity-based control [10-12], conventional sliding mode control [13-16], and continuous sliding mode control without chattering [17-21]. The aforementioned methods were able to provide satisfactory performances in terms of good tracking accuracy under the effects of model uncertainties and external disturbances to which an uncertain dynamic system might be subjected.

On the other hand, linear control approaches still remain the most popular and preferred options in handling robot control problems with the least computational cost. Among others, PD (proportional-derivative) or PID (proportional-integral-derivative) control is a traditional but powerful strategy that usually takes the information about the deviation of the actual state from the desired state and feeds it back into the plant input. Neither exact dynamic modeling nor complex calculation of input torques are necessary for the implementation of PD/PID control [22]. Hence, a good number of researchers and engineers have applied PD/PID control to robot manipulator trajectory tracking [23-25]. Kawamura et al. [22] developed a local PD feedback controller with gravity compensation that forces a robot manipulator to follow a desired reference trajectory with arbitrary accuracy if the velocity feedback gain is set sufficiently large and the initial position/velocity errors are sufficiently small. It is known that unlike PD control, classical PID control reduces a bandwidth of the closed-loop system and guarantees only semiglobal stability that yields arbitrary small output tracking errors from a given set of initial conditions [26, 27]. Hence, Arimoto [28] and Kelly [29] added nonlinear integral terms to a linear PD feedback law to ensure global asymptotic stability. Cervantes and Alvarez-Ramirez [27] proposed a method of selecting PID control gains such that the tracking error should be sufficiently small for any compact set of initial position and velocity errors. The problem was solved by considering the closed-loop system as a standard singularly perturbed nonlinear system where all nonlinearities were lumped into a single function and estimated via a reduced-order observer. They assumed that the upper and lower bounds of the inertia matrix are a priori known. Jafarov et al. [30] developed a variable structure PID control law with a PID sliding surface that achieves global asymptotic stability of the controlled robot system. However, the bounds on the system parameter matrices were again assumed to be known. Nunes and Hsu [31] proposed a causal PD controller plus a feedforward compensation that yields uniform global asymptotic stability with respect to bounded input disturbances and derived inequality conditions for the PD control gains. However, the robot dynamic model was assumed to be known in advance in their method. Some researchers considered saturated torque constraints in their studies. Gorez [32] was the first who presented a bounded PID control law for global regulation assuming these kinds of constraints. Since the control scheme proposed in [32] was quite complex, Su et al. [33] attempted to obtain simpler structures, a so-called SP-SI-SD algorithm through Lyapunov stability analysis. Mendoza et al. [34] further simplified this algorithm and developed an output-feedback



scheme by creating a velocity estimated auxiliary subsystem.

Most robust controllers of robot manipulators in the literature are nonadaptive and possess time-invariant control laws. They are usually obtained by assuming that the upper and lower bounds on the model uncertainties or disturbances are a priori known. However, an accurate estimation of these bounds is difficult or costly to obtain in practice when controlling a time-varying nonlinear model of a robot manipulator in an unknown environment. Hence, adaptive control that automatically tunes its control parameters has also been studied to increase the flexibility in handling the time-varying nature of uncertain dynamics and disturbances. Tomei [35] designed a partially adapted PD controller that is adaptive with reference to unknown gravity parameters and ensures global asymptotic stability for any initial position/velocity errors. However, only a gravity term was estimated via adaptive dynamics and it was assumed that the bounds on the inertia and friction matrices are available in advance. Burkan [36] derived a parameter estimation law in terms of trigonometric functions and designed an adaptive PD controller with feedforward terms. The controller was obtained based on so-called linearly-in-parameter conditions such that the robot dynamics is assumed to be linear with uncertain constant inertia parameters. However, some drawbacks in the control performance, such as large overshoots or long settling time could be noticed. Xu and Qiao [37] combined a constant-gain PID control law with a robust adaptive algorithm that estimates the uncertain masses and the upper bounds on the disturbances to achieve global asymptotic trajectory tracking. However, the main limitation lies in the requirement that the D gain and the I gain should be identical, which constrains the flexibility of the controller and also chattering can be observed in the control signals. Nohooji [38] developed a self-tuning PID scheme in conjunction with neural networks for trajectory tracking of robot manipulators subject to uncertain dynamics and disturbances. The resulting controller was further improved by introducing a barrier Lyapunov function to prevent the violation of constraints and uniform boundedness of all signals is achieved in the closed-loop system. However, the learning of neural networks is computationally heavy and designing control and neural network parameters needs experience in control design. Thus, there is a strong demand to develop a simple adaptive PD/PID control law with the least computational cost that can be easily used even with little information about the uncertain dynamics of a robot manipulator to be controlled.

Motivated by the considerations above, the current paper proposes a simple adaptive PD control (APDC) scheme that achieves high-precision trajectory tracking of robot manipulators facing unknown dynamics and external disturbances. The control law is designed based on a simple self-tuning PD structure that automatically updates its gain and renders the tracking errors uniformly ultimately bounded within a prespecified small domain around the origin from nonzero initial errors. The proposed control approach captures advantages from both linear control and robust control and mainly aims at achieving high tracking accuracy while keeping its structure as simple as possible. The main contributions of this work can be summarized as follows:

1. The APDC guarantees uniform ultimate boundedness of the tracking errors with little information about the uncertain manipulator dynamics and external disturbances that are time varying. Only an estimate of the inertia matrix is needed and it is shown that the tracking accuracy is less sensitive to the choice of the estimate. Performance comparison with an existing nonlinear sliding mode controller is also conducted in terms of tracking accuracy, control effort, and computational cost.
2. Compared with the existing PD/PID controllers for robotic systems in the literature that frequently assumed the linearly-in-parameter conditions [31, 36, 37], the current paper directly deals with the usual nonlinear dynamics of robot manipulators with model uncertainties and external disturbances. Also, unlike most existing adaptive controllers that involve complex coupled conditions for control parameters to be satisfied, only one parameter is adaptive in the control algorithm and the control parameters can be selected independently by having simple inequality conditions satisfied.
3. The APDC proposed in this paper is of a pure PD form that consists of only position and velocity tracking errors with adaptive gains, whereas other existing PD/PID controllers for robotic systems usually have additional nonlinear terms to guarantee stability or boundedness of the signals generated by the controlled system [28-35, 37]. Since it has a simple PD structure, the presented control method preserves many benefits of linear control techniques such as easy design, stability study, and frequency-domain analysis.
4. Since the design of the control and adaptation laws boils down to the selection of control parameters, brief guidelines of how to select good parameters to achieve desired performance are provided. In addition, the effects of each parameter on tracking accuracy and control effort are investigated.

This paper is organized as follows. In Section 2 the nonlinear dynamic model of a robot manipulator and the proposed APDC scheme are provided. Then stability analysis of the controlled system is conducted in Section 3, followed by simulation verifications for tracking problems under various conditions in Section 4. Comparison with an existing nonlinear sliding mode controller and the effects of each control parameter on control performance are also discussed. Finally, Section 5 concludes this paper.

2. Dynamic Model and Adaptive PD Control Law

The dynamic model of a n -degree-of-freedom robot manipulator is described as a second-order nonlinear system as follows [25]:

$$\mathbf{M}(\mathbf{q})\ddot{\mathbf{q}} + \mathbf{C}(\mathbf{q},\dot{\mathbf{q}})\dot{\mathbf{q}} + \mathbf{G}(\mathbf{q}) = \boldsymbol{\tau}(t) + \mathbf{d}(t), \tag{1}$$

where $\mathbf{q}(t)$ is the n by 1 vector of the joint coordinates, $\mathbf{M}(\mathbf{q})$ is the n by n inertia matrix which is positive definite, $\mathbf{C}(\mathbf{q},\dot{\mathbf{q}})$ is the n by n matrix that stands for the Coriolis and centrifugal forces, $\mathbf{G}(\mathbf{q})$ is the n by 1 vector of gravity forces, $\boldsymbol{\tau}(t)$ is the n by 1 vector of the applied torques, $\mathbf{d}(t)$ is the n by 1 vector of the external disturbances, and t denotes time. The block diagram of the controlled robot manipulator system is provided in Fig. 1. It is assumed that the dynamic model eq. (1) includes model uncertainties. Hence, actual (unknown) values of these quantities can be denoted as $\mathbf{M}(\mathbf{q}) = \mathbf{M}_0(\mathbf{q}) + \Delta\mathbf{M}(\mathbf{q})$, $\mathbf{C}(\mathbf{q},\dot{\mathbf{q}}) = \mathbf{C}_0(\mathbf{q},\dot{\mathbf{q}}) + \Delta\mathbf{C}(\mathbf{q},\dot{\mathbf{q}})$, and $\mathbf{G}(\mathbf{q}) = \mathbf{G}_0(\mathbf{q}) + \Delta\mathbf{G}(\mathbf{q})$, where the notations $\mathbf{M}_0(\mathbf{q})$, $\mathbf{C}_0(\mathbf{q},\dot{\mathbf{q}})$, and $\mathbf{G}_0(\mathbf{q})$ stand for the nominal matrices that are known, and $\Delta\mathbf{M}(\mathbf{q})$, $\Delta\mathbf{C}(\mathbf{q},\dot{\mathbf{q}})$, and $\Delta\mathbf{G}(\mathbf{q})$ denote the model uncertainties. In what follows, the arguments of the various quantities will be suppressed unless required for clarity. Consequently, eq. (1) can be rewritten as

$$\mathbf{M}_0\ddot{\mathbf{q}} + \mathbf{C}_0\dot{\mathbf{q}} + \mathbf{G}_0 = \boldsymbol{\tau} + \mathbf{d} + \mathbf{F}_d, \tag{2}$$

where

$$\mathbf{F}_d \triangleq -\Delta\mathbf{M}\ddot{\mathbf{q}} - \Delta\mathbf{C}\dot{\mathbf{q}} - \Delta\mathbf{G} \tag{3}$$

is the total lumped system uncertainty. We succinctly express eq. (2) in the acceleration level as



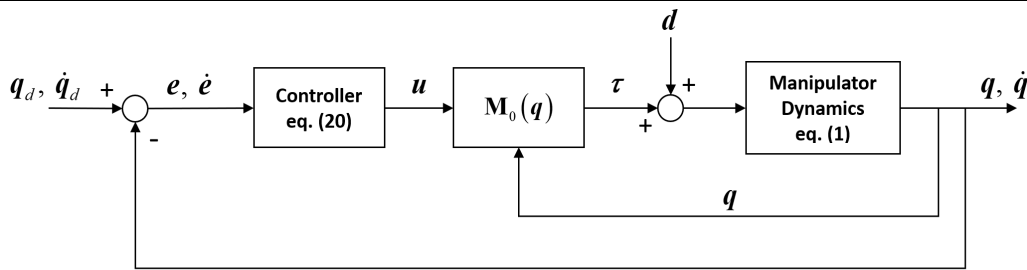


Fig. 1. Block diagram of the controlled robot manipulator system

$$\ddot{q} = \mathbf{M}_0^{-1}\tau + \mathbf{M}_0^{-1}(-\mathbf{C}_0\dot{q} - \mathbf{G}_0 + d + F_d) = \mathbf{u} + \Delta, \tag{4}$$

where the control acceleration vector \mathbf{u} and the uncertain term Δ are defined as

$$\mathbf{u} \triangleq \mathbf{M}_0^{-1}\tau, \quad \Delta \triangleq \mathbf{M}_0^{-1}(-\mathbf{C}_0\dot{q} - \mathbf{G}_0 + d + F_d). \tag{5}$$

Let us define the tracking error vector as

$$\mathbf{e}(t) = \mathbf{q}(t) - \mathbf{q}_d(t), \tag{6}$$

where $\mathbf{q}_d(t) = [q_{d,1}(t) \quad q_{d,2}(t) \quad \dots \quad q_{d,n}(t)]^T$ is the desired position vector. If we differentiate eq. (6) with respect to time twice, we have

$$\ddot{\mathbf{e}} = \ddot{\mathbf{q}} - \ddot{\mathbf{q}}_d = \mathbf{u} + \boldsymbol{\gamma}, \tag{7}$$

where eq. (4) is used and $\boldsymbol{\gamma} \triangleq \Delta - \ddot{\mathbf{q}}_d$ is defined. In the current paper, it is assumed that the uncertain term $\boldsymbol{\gamma}$ is bounded by

$$\|\boldsymbol{\gamma}\|_\infty \triangleq \max(|\gamma_1|, |\gamma_2|, \dots, |\gamma_n|) < \Gamma, \tag{8}$$

where $\|\cdot\|_\infty$ is the infinity-norm of a vector and Γ is an unknown positive constant.

Let us consider the following control law:

$$\mathbf{u} = -2\zeta\omega_n\dot{\mathbf{e}} - \omega_n^2\mathbf{e} + \mathbf{v} = -2\zeta\omega_n(\dot{\mathbf{q}} - \dot{\mathbf{q}}_d) - \omega_n^2(\mathbf{q} - \mathbf{q}_d) + \mathbf{v}, \tag{9}$$

where ζ and ω_n are positive constants to be selected by the user and $\mathbf{v}(t)$ is an auxiliary control function to be designed. As can be easily deduced, ζ and ω_n will act as the damping ratio and the natural frequency of the controlled system, which determine the transient response from the initial conditions. Substituting eq. (9) into eq. (7), we obtain

$$\ddot{\mathbf{e}} + 2\zeta\omega_n\dot{\mathbf{e}} + \omega_n^2\mathbf{e} = \mathbf{v} + \boldsymbol{\gamma}. \tag{10}$$

It is straightforward to see that while the additional control input $\mathbf{v}(t)$ fights for the uncertainty $\boldsymbol{\gamma}(t)$ to suppress its effect on the system and the right hand side of eq. (10) remains sufficiently small so that $\mathbf{v} + \boldsymbol{\gamma} \approx \mathbf{0}$, the first two terms of $\mathbf{u}(t)$ in eq. (9) make the errors $\mathbf{e}(t)$ decay exponentially because $\ddot{\mathbf{e}} + 2\zeta\omega_n\dot{\mathbf{e}} + \omega_n^2\mathbf{e} \rightarrow \mathbf{0}$ as $t \rightarrow \infty$. In the current paper, to minimize control effort the control torque is assumed to be subjected to a saturation limit so that

$$\|\boldsymbol{\tau}(t)\|_\infty \leq T^*, \tag{11}$$

where T^* is a known positive value. Since $\mathbf{u} = \mathbf{M}_0^{-1}\boldsymbol{\tau}$, the control acceleration is bounded by

$$\|\mathbf{u}(t)\|_\infty = \|\mathbf{M}_0^{-1}(\mathbf{q})\boldsymbol{\tau}(t)\|_\infty \leq \|\mathbf{M}_0^{-1}(\mathbf{q})\|_\infty \|\boldsymbol{\tau}(t)\|_\infty \leq \|\mathbf{M}_0^{-1}(\mathbf{q})\|_\infty T^* \triangleq U^*, \tag{12}$$

where $\|\mathbf{M}_0^{-1}(\mathbf{q})\|_\infty$ is the maximum absolute row sum of the matrix $\mathbf{M}_0^{-1}(\mathbf{q})$, which is the matrix norm induced by the infinity norm on vectors. Since $\mathbf{M}_0(\mathbf{q})$ is a known matrix, the upper bound U^* in eq. (12) can be calculated.

Now, we rewrite eq. (10) using the state-space representation as follows:

$$\begin{bmatrix} \dot{\mathbf{e}} \\ \ddot{\mathbf{e}} \end{bmatrix} = \begin{bmatrix} \mathbf{0}_{n \times n} & \mathbf{I}_{n \times n} \\ -\omega_n^2\mathbf{I}_{n \times n} & -2\zeta\omega_n\mathbf{I}_{n \times n} \end{bmatrix} \begin{bmatrix} \mathbf{e} \\ \dot{\mathbf{e}} \end{bmatrix} + \begin{bmatrix} \mathbf{0}_{n \times n} \\ \mathbf{I}_{n \times n} \end{bmatrix} (\mathbf{v} + \boldsymbol{\gamma}), \tag{13}$$

or

$$\dot{\boldsymbol{\varepsilon}} = \mathbf{A}\boldsymbol{\varepsilon} + \mathbf{B}(\mathbf{v} + \boldsymbol{\gamma}), \tag{14}$$

where

$$\boldsymbol{\varepsilon} \triangleq \begin{bmatrix} \mathbf{e} \\ \dot{\mathbf{e}} \end{bmatrix}, \quad \mathbf{A} \triangleq \begin{bmatrix} \mathbf{0}_{n \times n} & \mathbf{I}_{n \times n} \\ -\omega_n^2\mathbf{I}_{n \times n} & -2\zeta\omega_n\mathbf{I}_{n \times n} \end{bmatrix}, \quad \mathbf{B} = \begin{bmatrix} \mathbf{0}_{n \times n} \\ \mathbf{I}_{n \times n} \end{bmatrix}. \tag{15}$$

Here, $\mathbf{0}_{n \times n}$ and $\mathbf{I}_{n \times n}$ denote the n by n zero matrix and the n by n identity matrix, respectively.

The aim is to find the additional control input \mathbf{v} such that the error vector $\boldsymbol{\varepsilon}$ in eq. (14) decays to zero (or to within a sufficiently small domain) as time goes by despite the presence of the uncertain term $\boldsymbol{\gamma}$ which is time varying but bounded. We



propose the following robust adaptive PD control law $v(t)$ in eq. (9) for tracking control of an uncertain robot manipulator system:

$$v(t) = -\frac{K(t)}{\delta} \left[\dot{e}(t) + \frac{\omega_n}{2\zeta} e(t) \right] = -\frac{K(t)}{\delta} h(t), \tag{16}$$

where $h(t) \triangleq \dot{e}(t) + \omega_n e(t) / 2\zeta$ and $\delta > 0$ is a constant to be selected by the user that determines control accuracy as shall be shown shortly. Also, $K(t)$ is the control gain that is updated by the following adaptation law:

$$\dot{K}(t) = \eta \left[\|v(t)\|_\infty - K(t) + K_0 \right] = \eta \left[\left(\frac{\|h(t)\|_\infty}{\delta} - 1 \right) K(t) + K_0 \right], \quad (K(0) \geq K_0) \tag{17}$$

where $\eta > 0$ and $K_0 > 0$ are control parameters to be selected by the user. The value of η is selected to prevent a sudden rise of the gain and K_0 offers additional stability margin. It is noted that the condition $K(t) \geq K_0 > 0$ is always satisfied. Since $\|v(t)\|_\infty \geq 0$, eq. (17) then becomes

$$\dot{K} \geq \eta (-K + K_0). \tag{18}$$

Defining $L(t) \triangleq K(t) - K_0$, we have $\dot{L}(t) \geq -\eta L(t)$ and hence,

$$L(t) \geq L(0) e^{-\eta t} = L(0) e^{-\eta t} \geq 0, \tag{19}$$

where the Gronwall's inequality [39] is used. Since $L(t) \geq 0$, the condition $K(t) \geq K_0 > 0$ holds and the gain $K(t)$ is always positive.

Then, the overall control law $u(t)$ is obtained by substituting eq. (16) into eq. (9) and we obtain

$$u(t) = -2\zeta\omega_n \left[\dot{e}(t) + \frac{\omega_n}{2\zeta} e(t) \right] - \frac{K(t)}{\delta} \left[\dot{e}(t) + \frac{\omega_n}{2\zeta} e(t) \right] = -\left(2\zeta\omega_n + \frac{K(t)}{\delta} \right) \left[\dot{e}(t) + \frac{\omega_n}{2\zeta} e(t) \right] \tag{20}$$

with the gain adaptation rule eq. (17). It must be noted that the proposed adaptive PD control law eq. (20) includes only the tracking errors and their time derivatives. We now propose the main theorem.

Theorem: Consider the robot manipulator system eq. (1) or eq. (4) with the adaptive PD control (APDC) law eq. (20) and the gain adaptation rule eq. (17). Then, the controlled system will be stable such that the errors are uniformly ultimately bounded by $\|e(t)\|_\infty \leq 2\zeta\delta\omega_n$ in a finite time from any nonzero initial errors, provided that the control parameters are selected as follows:

$$\begin{cases} \omega_n > 0, \delta > 0, \eta > 0, K(0) \geq K_0 > 0, \\ \frac{1}{2} < \zeta, \\ K(0) + 2\zeta\omega_n\delta < U^*. \end{cases} \tag{21}$$

The proof of Theorem is given in the next section.

3. Stability Analysis

Before we prove Theorem in the previous section, let us first prove the following two Lemmas.

Lemma 1: Let us consider the following $2n$ by $2n$ symmetric matrix:

$$P = \begin{bmatrix} 2\omega_n^2 I_{n \times n} & \frac{\omega_n}{2\zeta} I_{n \times n} \\ \frac{\omega_n}{2\zeta} I_{n \times n} & I_{n \times n} \end{bmatrix}, \tag{22}$$

where ζ and ω_n are constants satisfying the conditions eq. (21) and a $2n$ by $2n$ symmetric matrix Q is defined as $Q = -(A^T P + P A)$ where A is the matrix defined in eq. (15). Then both matrices P and Q are positive definite.

Proof: First, the matrix P is positive definite if and only if the following conditions are satisfied [40]:

$$2\omega_n^2 > 0, \quad \frac{\omega_n^2}{4\zeta^2} (8\zeta^2 - 1) > 0. \tag{23}$$

The two conditions in eq. (23) are immediately derived from eq. (21).

Next, we show the positive definiteness of the matrix Q . From its definition, we can easily compute the matrix Q as

$$Q = -(A^T P + P A) = \begin{bmatrix} \frac{\omega_n^3}{\zeta} I_{n \times n} & \mathbf{0}_{n \times n} \\ \mathbf{0}_{n \times n} & \frac{\omega_n}{\zeta} (4\zeta^2 - 1) I_{n \times n} \end{bmatrix}. \tag{24}$$

Then from the conditions eq. (21), it is obvious that the matrix Q is positive definite, which completes the proof. ■



Lemma 2: Assume that the magnitude of the control input $u(t)$ given in eq. (20) is subjected to a saturation limit U^* as described in eq. (12). Then, the gain $K(t)$ updated by the adaptive rule eq. (17) is always less than the value of $U^* - 2\zeta\omega_n\delta$ when $\|h(t)\|_\infty = \|\dot{e}(t) + \omega_n e(t) / 2\zeta\|_\infty > \delta$ holds. In brief, the following inequality is satisfied:

$$0 < K_0 \leq K(t) < U^* - 2\zeta\omega_n\delta, \text{ when } \|h(t)\|_\infty > \delta. \tag{25}$$

Proof: From eq. (20), we have

$$\|u(t)\|_\infty = \frac{2\zeta\omega_n\delta + K(t)}{\delta} \|h(t)\|_\infty, \tag{26}$$

since $K(t) > 0$ for all time t . Then, when $\|h(t)\|_\infty > \delta$, eq. (26) leads to

$$2\zeta\omega_n\delta + K(t) < \frac{2\zeta\omega_n\delta + K(t)}{\delta} \|h(t)\|_\infty = \|u(t)\|_\infty \leq U^*, \tag{27}$$

and since $0 < K_0 \leq K(t)$ and $K_0 \leq K(0)$, eq. (25) follows. ■

Now, we are ready to prove Theorem. Define a Lyapunov candidate function as

$$V = \frac{1}{2} \varepsilon^T P \varepsilon + \frac{\delta}{2\eta K_0} (K - K^*)^2, \tag{28}$$

where K^* is a sufficiently large number such that $\Gamma < K^*$ and $U^* < K^*$ are satisfied. The time derivative of eq. (28) yields

$$\dot{V} = \frac{1}{2} (\dot{\varepsilon}^T P \varepsilon + \varepsilon^T P \dot{\varepsilon}) + \frac{\delta}{\eta K_0} (K - K^*) \dot{K}. \tag{29}$$

Upon using eq. (14), eq. (29) becomes

$$\dot{V} = \frac{1}{2} \varepsilon^T (A^T P + P A) \varepsilon + \varepsilon^T P B (v + \gamma) + \frac{\delta}{\eta K_0} (K - K^*) \dot{K}. \tag{30}$$

Since $A^T P + P A = -Q$ from Lemma 1 and

$$\varepsilon^T P B = \begin{bmatrix} e^T & \dot{e}^T \end{bmatrix} \begin{bmatrix} 2\omega_n^2 \mathbf{I}_{n \times n} & \frac{\omega_n}{2\zeta} \mathbf{I}_{n \times n} \\ \frac{\omega_n}{2\zeta} \mathbf{I}_{n \times n} & \mathbf{I}_{n \times n} \end{bmatrix} \begin{bmatrix} \mathbf{0}_{n \times n} \\ \mathbf{I}_{n \times n} \end{bmatrix} = \frac{\omega_n}{2\zeta} e^T + \dot{e}^T = h^T \tag{31}$$

from eqs. (15) and (22), eq. (30) simplifies to

$$\dot{V} = -\frac{1}{2} \varepsilon^T Q \varepsilon + h^T (v + \gamma) + \frac{\delta}{\eta K_0} (K - K^*) \dot{K} = -\frac{1}{2} \varepsilon^T Q \varepsilon + \dot{V}_K, \tag{32}$$

where $\dot{V}_K \triangleq h^T (v + \gamma) + \frac{\delta}{\eta K_0} (K - K^*) \dot{K}$. Substituting eqs. (8) and (16) into \dot{V}_K , we obtain

$$\dot{V}_K < \|h\|_\infty \left(\Gamma - \frac{K}{\delta} h^T h + \frac{\delta}{\eta K_0} (K - K^*) \dot{K} \right) \leq \|h\|_\infty \left(\Gamma - \frac{K}{\delta} \|h\|_\infty \right) + \frac{\delta}{\eta K_0} (K - K^*) \dot{K} \tag{33}$$

since $\|h\|_\infty^2 \leq h^T h$. Now, let us consider the case when $\|h\|_\infty > \delta$. Then, from eq. (33) we have

$$\begin{aligned} \dot{V}_K &< \|h\|_\infty (\Gamma - K) + \frac{\delta}{\eta K_0} (K - K^*) \dot{K} = \|h\|_\infty (\Gamma - K) + \frac{\delta}{\eta K_0} (K - K^*) \dot{K} + \|h\|_\infty (K^* - K) - \|h\|_\infty (K^* - K) \\ &= \|h\|_\infty (\Gamma - K^*) - \frac{\delta}{\eta K_0} (K^* - K) \dot{K} + \|h\|_\infty (K^* - K) = -\|h\|_\infty (K^* - \Gamma) - (K^* - K) \left(\frac{\delta}{\eta K_0} \dot{K} - \|h\|_\infty \right). \end{aligned} \tag{34}$$

Since $K^* > \Gamma$, the first term in eq. (34) is negative. Substituting eq. (17) into the second term, we have

$$\dot{V}_K < -(K^* - K) \left(\frac{\delta}{\eta K_0} \dot{K} - \|h\|_\infty \right) = -(K^* - K) \left[\frac{\delta}{K_0} \left(\left(\frac{\|h\|_\infty}{\delta} - 1 \right) K + K_0 \right) - \|h\|_\infty \right] = -(K^* - K) \frac{K - K_0}{K_0} (\|h\|_\infty - \delta) \leq 0 \tag{35}$$

because $K^* > K$, $K \geq K_0$, and $\|h\|_\infty > \delta$. Hence, $\dot{V}_K < 0$ and eq. (32) becomes

$$\dot{V} = -\frac{1}{2} \varepsilon^T Q \varepsilon + \dot{V}_K < -\frac{1}{2} \varepsilon^T Q \varepsilon < 0 \tag{36}$$

since the matrix Q is positive definite. In brief, if we define a compact set Ω_δ such that $\|h\|_\infty = \|\dot{e} + e\omega_n / 2\zeta\|_\infty \leq \delta$, then all the solutions of $h(t)$ that start outside Ω_δ will enter this set within a finite time and will remain inside the set for all future times [41].



While the errors and their derivatives remain inside the set Ω_δ , each element satisfies

$$-\delta \leq \dot{e}_i + \frac{\omega_n}{2\zeta} e_i \leq \delta, \quad i = 1, 2, \dots, n. \tag{37}$$

First, consider the case $\dot{e}_i + \omega_n e_i / 2\zeta \leq \delta$ or $\dot{e}_i \leq -\omega_n (e_i - 2\zeta\delta / \omega_n) / 2\zeta$. Then, using the Gronwall's inequality [39], we can easily show that

$$e_i(t) \leq \frac{2\zeta\delta}{\omega_n} + \left[e_i(t_0) - \frac{2\zeta\delta}{\omega_n} \right] e^{-\frac{\omega_n}{2\zeta}(t-t_0)}, \tag{38}$$

where t_0 is the time instant at which the condition $|\dot{e}_i + \omega_n e_i / 2\zeta| \leq \delta$ is first satisfied, and $t \geq t_0 \geq 0$. Since $\omega_n / 2\zeta > 0$, the error $e_i(t)$ is ultimately bounded by $e_i(t) \leq 2\zeta\delta / \omega_n$. Next, we consider the case $-\delta \leq \dot{e}_i + \omega_n e_i / 2\zeta$ or $-\delta - \omega_n e_i / 2\zeta \leq \dot{e}_i$. Following the same procedure as in the first case, we arrive at

$$-\frac{2\zeta\delta}{\omega_n} + \left[e_i(t_0) + \frac{2\zeta\delta}{\omega_n} \right] e^{-\frac{\omega_n}{2\zeta}(t-t_0)} \leq e_i(t), \tag{39}$$

and the error $e_i(t)$ is ultimately bounded by $-2\zeta\delta / \omega_n \leq e_i(t)$. Hence, we combine the two results such that

$$-\frac{2\zeta\delta}{\omega_n} \leq e_i(t) \leq \frac{2\zeta\delta}{\omega_n}, \tag{40}$$

and eq. (40) is satisfied for any element $i = 1, 2, \dots, n$, and so we conclude that

$$\|e(t)\|_\infty \leq \frac{2\zeta\delta}{\omega_n}. \tag{41}$$

This is the end of the proof. ■

4. Simulation Results

The adaptive PD control (APDC) law developed in the previous sections is applied to trajectory tracking of the 2-link robot manipulators shown in Fig. 2 to validate its effectiveness, accuracy, and robustness, and compared with the existing nonlinear sliding mode controller proposed in [15]. The simulations are carried out in the MATLAB/Simulink environment, using the fixed-step ode4 Runge-Kutta integrator with the sampling interval of 0.001 sec.

In this paper, the same nonlinear dynamic equation of the manipulator as used by Boukattaya et al. [15] is considered for performance comparison:

$$\begin{bmatrix} M_{11}(q) & M_{12}(q) \\ M_{21}(q) & M_{22}(q) \end{bmatrix} \begin{bmatrix} \ddot{q}_1 \\ \ddot{q}_2 \end{bmatrix} + \begin{bmatrix} C_{11}(q, \dot{q}) & C_{12}(q, \dot{q}) \\ C_{21}(q, \dot{q}) & C_{22}(q, \dot{q}) \end{bmatrix} \begin{bmatrix} \dot{q}_1 \\ \dot{q}_2 \end{bmatrix} + \begin{bmatrix} G_1(q) \\ G_2(q) \end{bmatrix} = \begin{bmatrix} \tau_1 \\ \tau_2 \end{bmatrix} + \begin{bmatrix} d_1 \\ d_2 \end{bmatrix}, \tag{42}$$

where

$$\begin{aligned} M_{11}(q) &= (m_1 + m_2)l_1^2 + m_2l_2^2 + 2m_2l_1l_2 \cos(q_2) + J_1, & M_{12}(q) &= M_{21}(q) = m_2l_2^2 + m_2l_1l_2 \cos(q_2), & M_{22}(q) &= m_2l_2^2 + J_2, \\ C_{11}(q, \dot{q}) &= -2m_2l_1l_2 \sin(q_2)\dot{q}_2, & C_{12}(q, \dot{q}) &= -m_2l_1l_2 \sin(q_2)\dot{q}_2, & C_{21}(q, \dot{q}) &= m_2l_1l_2 \sin(q_2)\dot{q}_1, & C_{22}(q, \dot{q}) &= 0, \\ G_1(q) &= (m_1 + m_2)gl_1 \cos(q_1) + m_2gl_2 \cos(q_1 + q_2), & G_2(q) &= m_2gl_2 \cos(q_1 + q_2). \end{aligned} \tag{43}$$

The nominal parameters are selected as

$$\hat{l}_1 = 1 \text{ m}, \hat{l}_2 = 0.8 \text{ m}, \hat{m}_1 = 0.5 \text{ kg}, \hat{m}_2 = 1.5 \text{ kg}, \hat{J}_1 = 5 \text{ kg} \cdot \text{m}^2, \hat{J}_2 = 5 \text{ kg} \cdot \text{m}^2, \tag{44}$$

where q_i ($i = 1, 2$) is the angular position of the revolute joint i , l_i is the length of link i , m_i is the mass of link i , J_i is the inertia of link i , respectively, and $g = 9.81 \text{ m/s}^2$ is the acceleration due to gravity. Note that the known terms \hat{l}_1 , \hat{l}_2 , \hat{m}_1 , \hat{m}_2 , \hat{J}_1 , and \hat{J}_2 determine the nominal matrices $\mathbf{M}_0(q)$, $\mathbf{C}_0(q, \dot{q})$, and $\mathbf{G}_0(q)$ used in eq. (2). The desired trajectories are selected as

$$q_d = \begin{bmatrix} q_{d,1} \\ q_{d,2} \end{bmatrix} = \begin{bmatrix} 1.25 - \frac{7}{5}e^{-t} + \frac{7}{20}e^{-4t} \\ 1.25 + e^{-t} + \frac{1}{4}e^{-4t} \end{bmatrix}, \tag{45}$$

and the initial conditions are

$$q(0) = \begin{bmatrix} 1 \\ 1.5 \end{bmatrix} \text{ (rad)}, \dot{q}(0) = \begin{bmatrix} 0 \\ 0 \end{bmatrix} \text{ (rad/s)}. \tag{46}$$



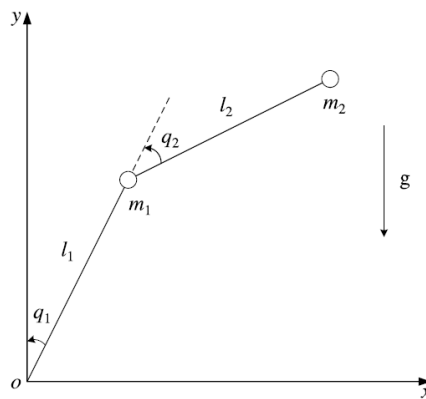


Fig. 2. Architecture of the two-link robot manipulator

The following external disturbances including high-frequency noise effects are applied to the manipulator:

$$d(t) = \begin{bmatrix} d_1(t) \\ d_2(t) \end{bmatrix} = \begin{bmatrix} 2 \sin(t) + 0.5 \sin(200\pi t) \\ \cos(2t) + 0.5 \sin(200\pi t) \end{bmatrix}, \tag{47}$$

and it is assumed that physical parameters of mass and inertia in eq. (42) are uncertain by 20 % of their nominal values such that the real values are

$$\begin{aligned} m_1 &= \hat{m}_1 + 0.2\hat{m}_1 = 0.6 \text{ kg}, \quad m_2 = \hat{m}_2 + 0.2\hat{m}_2 = 1.8 \text{ kg}, \\ J_1 &= \hat{J}_1 + 0.2\hat{J}_1 = 6 \text{ kg} \cdot \text{m}^2, \quad J_2 = \hat{J}_2 + 0.2\hat{J}_2 = 6 \text{ kg} \cdot \text{m}^2, \end{aligned} \tag{48}$$

where m_1 , m_2 , J_1 , and J_2 are the real, unknown values.

Now, let us consider the APDC described in Theorem. The parameters used for the controller are selected as

$$\delta = 0.005, \eta = 0.1, K_0 = 0.5, K(0) = 0.5, T^* = 4000. \tag{49}$$

As for the damping ratio ζ and the natural frequency ω_n in the left hand side of eq. (10) that determine the response of the controlled, linear dynamics, let us consider the following two cases:

$$\begin{aligned} \text{Case I: } & \zeta = 1, \omega_n = 5, \\ \text{Case II: } & \zeta = 0.67, \omega_n = 5, \end{aligned} \tag{50}$$

and both cases use the same control parameter values shown in eq. (49). It is obvious that Case I and Case II yield critically damped and underdamped responses, respectively. Also, the nominal mass matrix $\mathbf{M}_0(q)$ is calculated as

$$\mathbf{M}_0(q) = \begin{bmatrix} (\hat{m}_1 + \hat{m}_2)l_1^2 + \hat{m}_2l_2^2 + 2\hat{m}_2l_1l_2 \cos(q_2) + \hat{J}_1 & \hat{m}_2l_2^2 + \hat{m}_2l_1l_2 \cos(q_2) \\ \hat{m}_2l_2^2 + \hat{m}_2l_1l_2 \cos(q_2) & \hat{m}_2l_2^2 + \hat{J}_2 \end{bmatrix}. \tag{51}$$

Figure 3 plots the variation of $\|\mathbf{M}_0^{-1}(q)\|_\infty = \|\mathbf{M}_0^{-1}(q_2)\|_\infty$ as q_2 changes from 0 (rad) to 2π (rad). Since the maximum value of $\|\mathbf{M}_0^{-1}(q_2)\|_\infty$ is found to be 0.2193 at $q_2 = 0, 2\pi$ (rad), from eq. (12) $\|u(t)\|_\infty$ is bounded by $0.2193T^*$ such that $U^* = 0.2193T^* = 877.2$. Hence, all the conditions given in eq. (21) are met. If a constant nominal matrix $\mathbf{M}_0(q) = \mathbf{M}_0$ were selected, the calculation of U^* would have been a lot simpler. However, a time-varying $\mathbf{M}_0(q)$ was employed in this paper in order to show the general procedure to obtain U^* . Usually, the first and the second conditions in eq. (21) are immediately satisfied by selecting suitable positive parameters and the third condition is easily satisfied by selecting a sufficiently small δ that increases the tracking accuracy as shown by Theorem. The superiority of the conditions proposed in eq. (21) lies in their simplicity and the fact that the parameters can be chosen almost independently.

The simulation results in the presence of the uncertainties eq. (48) and the external disturbances eq. (47) are presented in Figs. 4 – 8 for both cases. The positions of joints 1 and 2 in comparison with the desired trajectories are illustrated in Fig. 4. The corresponding tracking error signals are shown in Fig. 5. It can be seen that Case II (underdamped) merges to the desired trajectories more quickly and the errors asymptotically decay at a desired rate specified by ζ and ω_n , and are ultimately bounded within the region $\|e(t)\|_\infty \leq 2\zeta\delta / \omega_n = 0.002$ for Case I and $\|e(t)\|_\infty \leq 2\zeta\delta / \omega_n = 0.00134$ for Case II, as indicated by Theorem. Figure 6 depicts the control torques for both cases and shows that the control signals are continuous and smooth. Large control torques are initially required for both cases but Case II requires even larger torques. The magnitude of the control torques at the initial time can explicitly be calculated by using eqs. (5), (20), (43), and (44) as

$$\tau(0) = \mathbf{M}_0 u(0) = - \begin{bmatrix} (\hat{m}_1 + \hat{m}_2)l_1^2 + \hat{m}_2l_2^2 + 2\hat{m}_2l_1l_2 \cos(q_2) + \hat{J}_1 & \hat{m}_2l_2^2 + \hat{m}_2l_1l_2 \cos(q_2) \\ \hat{m}_2l_2^2 + \hat{m}_2l_1l_2 \cos(q_2) & \hat{m}_2l_2^2 + \hat{J}_2 \end{bmatrix} \begin{bmatrix} \dot{e}_1(0) + \frac{\omega_n}{2\zeta} e_1(0) \\ \dot{e}_2(0) + \frac{\omega_n}{2\zeta} e_2(0) \end{bmatrix} = \begin{bmatrix} -1731.08 \\ 97.93 \end{bmatrix} \text{ N} \cdot \text{m} \text{ (Case I),} \tag{52}$$

$$\begin{bmatrix} -2396.37 \\ 768.21 \end{bmatrix} \text{ N} \cdot \text{m} \text{ (Case II),}$$



where $e(t) \triangleq [e_1(t) \ e_2(t)]^T$. In Fig. 7 the time history of the gains $K(t)$ for Cases I and II are depicted and both gains stay in a bounded region. Because of the *adaptive* mechanism of $K(t)$ good tracking performance is guaranteed even if exact information about the uncertainties is not a priori known. Figure 8 plots the time history of the control demand $v(t)$ calculated by eq. (16), the uncertainty term $\gamma(t)$ defined as $\gamma = A - \ddot{q}_d$ with eq. (5), and their sum $v(t) + \gamma(t)$ for both cases. It is noted that the control input $v(t)$ effectively eliminates the effect of the uncertainty $\gamma(t)$ so that the sum $v(t) + \gamma(t)$ remains a small value. Accordingly, one can expect from eq. (10) that the error $e(t)$ would asymptotically converge to a small domain, more specifically $\|e(t)\|_{\infty} \leq 2\zeta\delta / \omega_n$, at a desired rate characterized by the values of ζ and ω_n . Roughly speaking, the control parameters ζ and ω_n mainly determine the transient response while the steady-state response is also affected by the other parameters δ , η , and K_0 . Also, Case II yields a faster response and smaller steady-state errors than Case I, at the expense of larger control torques. Overall, the simulation results Figs. 4 – 8 corroborate great tracking performance and strong robustness of the proposed APDC against the model uncertainties and external disturbances.

In order to better demonstrate the excellence of the proposed APDC approach, another type of adaptive controller is now considered in the simulations for comparison, which is based on adaptive nonsingular fast terminal sliding mode control (ANFTSMC) proposed by Boukattaya et al. [15]. The sliding variable $s(t)$ and the adaptive control law $\tau(t)$ designed in [15] are given as

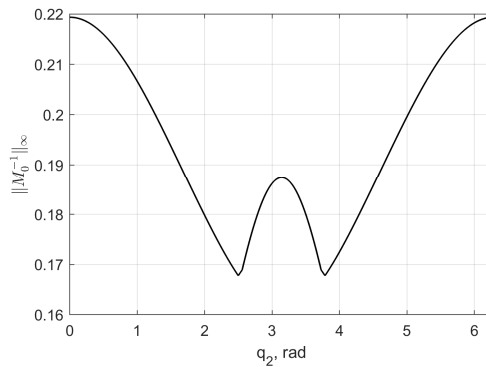


Fig. 3. Variation of $\|M_0^{-1}(q_2)\|_{\infty}$ as q_2 changes

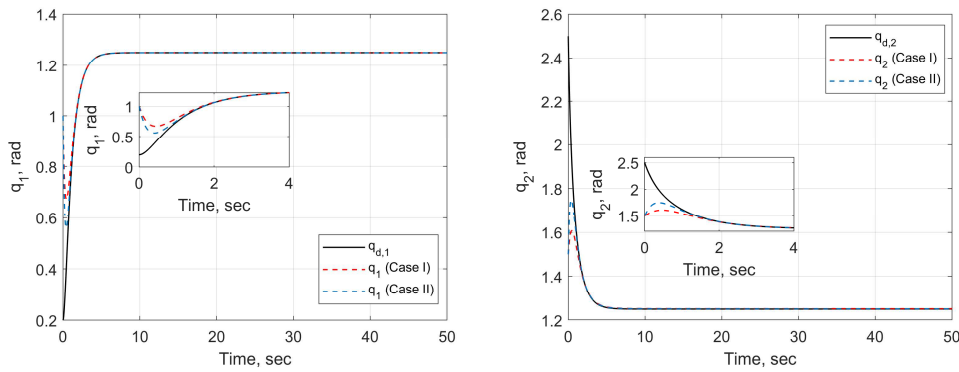


Fig. 4. Tracking responses of joints 1 (left) and 2 (right)

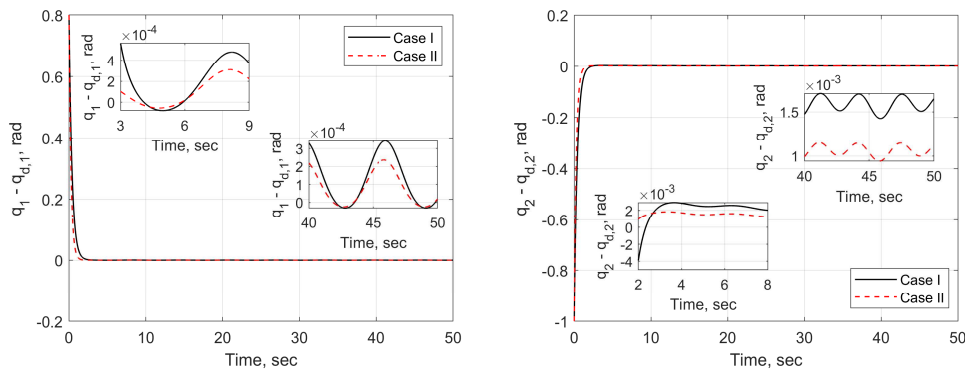


Fig. 5. Tracking errors of joints 1 (left) and 2 (right)



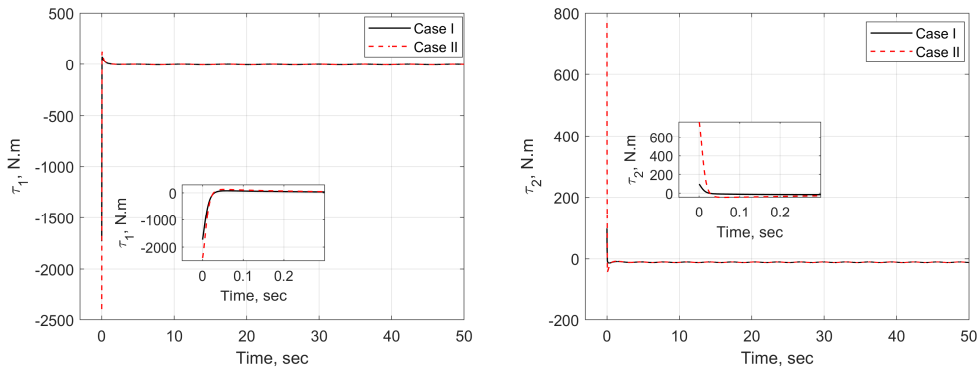


Fig. 6. Control input torques of joints 1 (left) and 2 (right)

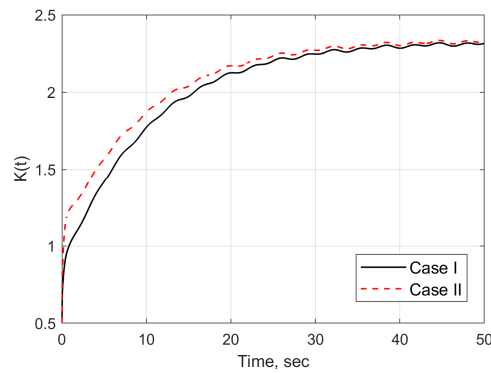


Fig. 7. Time history of gain $K(t)$

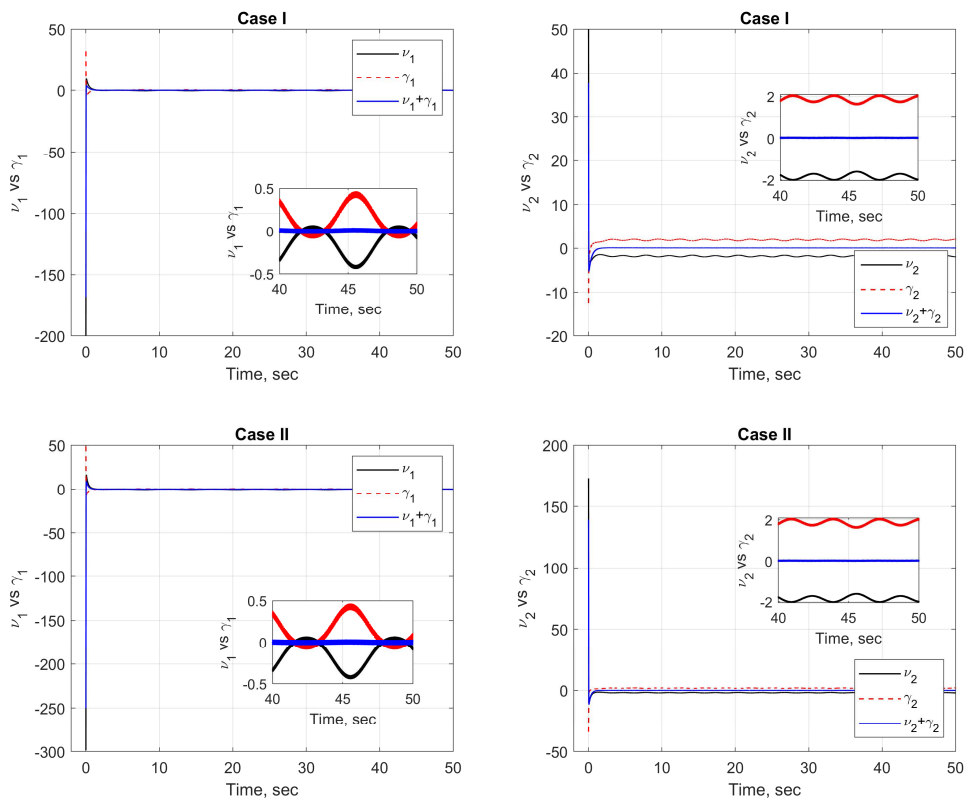


Fig. 8. Control input $\nu(t)$, uncertainty $\gamma(t)$, and the sum $\nu(t)+\gamma(t)$ of joints 1 (left) and 2 (right) for Case I (upper) and Case II (lower)



$$\begin{aligned}
 \mathbf{s} &= \mathbf{e} + k_1 |\mathbf{e}|^\alpha \operatorname{sgn}(\mathbf{e}) + k_2 |\dot{\mathbf{e}}|^\beta \operatorname{sgn}(\dot{\mathbf{e}}), \\
 \boldsymbol{\tau} &= \boldsymbol{\tau}_{eq} + \boldsymbol{\tau}_{asw}, \\
 \boldsymbol{\tau}_{eq} &= \mathbf{M}_0 \ddot{\mathbf{q}}_d + \mathbf{C}_0 \dot{\mathbf{q}} + \mathbf{G}_0 - \frac{1}{\beta k_2} \mathbf{M}_0 |\dot{\mathbf{e}}|^{2-\beta} \left(1 + \alpha k_1 |\mathbf{e}|^{\alpha-1}\right) \operatorname{sgn}(\dot{\mathbf{e}}), \\
 \boldsymbol{\tau}_{asw} &= -\mathbf{M}_0 \left[k \mathbf{s} + (\hat{\mathbf{b}}_0 + \hat{\mathbf{b}}_1 \|\mathbf{q}\| + \hat{\mathbf{b}}_2 \|\dot{\mathbf{q}}\|^2 + \xi) \operatorname{sgn}(\mathbf{s}) \right], \\
 \hat{\mathbf{b}}_0 &= \lambda_0 \|\mathbf{s}\| \|\dot{\mathbf{e}}\|^{\beta-1}, \hat{\mathbf{b}}_1 = \lambda_1 \|\mathbf{s}\| \|\dot{\mathbf{e}}\|^{\beta-1} \|\mathbf{q}\|, \hat{\mathbf{b}}_2 = \lambda_2 \|\mathbf{s}\| \|\dot{\mathbf{e}}\|^{\beta-1} \|\dot{\mathbf{q}}\|^2,
 \end{aligned}
 \tag{53}$$

where $1 < \beta < 2$, $\alpha > \beta$, and $k_1, k_2, k, \xi, \lambda_0, \lambda_1$, and λ_2 are positive constants. Also, for a real variable vector $\mathbf{x} = [x_1 \ x_2]^T$, its Euclidean norm is denoted by $\|\mathbf{x}\| = \sqrt{x_1^2 + x_2^2}$ and its fractional power is defined as

$$|\mathbf{x}|^\alpha \triangleq \begin{bmatrix} |x_1|^\alpha \\ |x_2|^\alpha \end{bmatrix}, \tag{54}$$

and

$$\operatorname{sgn}(\mathbf{x}) \triangleq \begin{bmatrix} \operatorname{sgn}(x_1) \\ \operatorname{sgn}(x_2) \end{bmatrix}, \tag{55}$$

where the signum function is defined as

$$\operatorname{sgn}(y) = \begin{cases} 1, & \text{if } y > 0 \\ 0, & \text{if } y = 0 \\ -1, & \text{if } y < 0 \end{cases} \tag{56}$$

for a real number y . The vectors \mathbf{q}, \mathbf{e} , and \mathbf{G}_0 and the matrices \mathbf{M}_0 and \mathbf{C}_0 in eq. (53) are defined in the same way as in this paper. In fact, Boukattaya et al. [15] solved exactly the same problem given in this section with the same initial conditions in the presence of the same model uncertainties and external disturbances, but using ANFTSMC. They selected the following control parameters to be used in eq. (53):

$$\alpha = 2, \beta = \frac{5}{3}, k_1 = k_2 = 1, k = 250, \xi = 0.5, \lambda_0 = \lambda_1 = \lambda_2 = 0.01, \hat{\mathbf{b}}_0(0) = \hat{\mathbf{b}}_1(0) = \hat{\mathbf{b}}_2(0) = 0. \tag{57}$$

It must be noticed that the ANFTSMC law described in eq. (53) requires precise knowledge of the nominal dynamic model of the controlled system (i.e., $\mathbf{M}_0, \mathbf{C}_0$, and \mathbf{G}_0) while the proposed APDC necessitates only \mathbf{M}_0 to construct $\boldsymbol{\tau} = \mathbf{M}_0 \mathbf{u}$. For industrial robots, the values for \mathbf{C}_0 are sometimes negligible, but the gravity terms in \mathbf{G}_0 are not. However, upon using the proposed APDC, the information about \mathbf{G}_0 is not needed thanks to the adaptive mechanism. Also, as shall be shown later, even a poor estimate of the nominal inertia matrix \mathbf{M}_0 still results in fairly good tracking accuracy. For quantitative comparison purpose, two indices are defined to measure the performance: the integral of the absolute values of the errors (IAE) and the integral of the absolute values of the control torques (IACT). The IAE is used as a numerical measure of the error tracking performance and the IACT shows the energy consumption [15]. They are defined for each joint as follows:

$$\text{IAE} \triangleq \int_0^{t_f} |\mathbf{e}(t)| dt, \tag{58}$$

$$\text{IACT} \triangleq \int_0^{t_f} |\boldsymbol{\tau}(t)| dt, \tag{59}$$

where t_f represents the total running time.

The tracking performance of each controller (APDC and ANFTSMC) is shown and compared in Fig. 9. As for the APDC, Case I (critically damped) using the parameters given in eqs. (49) and (50) was considered. It is observed that the proposed controller has faster convergence to the desired signals. This is also verified by Fig. 10 in which the errors in the satisfaction of the desired signals are depicted. Obviously, the proposed control law provides faster response than the nonlinear ANFTSMC approach shown in [15]. Figure 11 shows the time history of the control torques obtained by using each method. One can see from the zoomed-in graphs that the proposed APDC requires smaller control magnitude at the initial time and generates smooth control signals throughout the simulation while the sliding mode controller designed in [15] exhibits chattering because of the discontinuous signum function involved, which typically appears in sliding mode control. Table 1 presents the comparison of the performance indices, where it is clearly seen that the proposed control strategy yields smaller IAE and IACT values than the existing control method (except IACT for joint 2). In Table 1 one more performance index is added: computation time (CT). This index indicates the computation time to execute each control algorithm for the total running time ($t_f = 50$ sec) and is used as a measure of computational cost. The function ‘tic-toc’ in MATLAB was used and the execution for each algorithm was repeated multiple times so that the computation time results could be averaged. Obviously, the proposed linear APDC scheme requires more than four times shorter computation time than the nonlinear ANFTSMC proposed in [15]. Hence, it is concluded that the simple APDC method proposed in this paper requires low computational cost and yields a fast convergence rate, high-precision tracking, no chattering, and great robustness against model uncertainties and external disturbances whose upper bounds are not known a priori.

Table 1. Comparison of the performance indices

Controller	IAE (rad·s)		IACT (m·N·s)		CT (s)
	Joint 1	Joint 2	Joint 1	Joint 2	
Proposed Controller	0.3256	0.4776	227.0	564.7	1.8643
Boukattaya et al. Controller [15]	0.4222	0.5496	258.7	564.3	7.6010



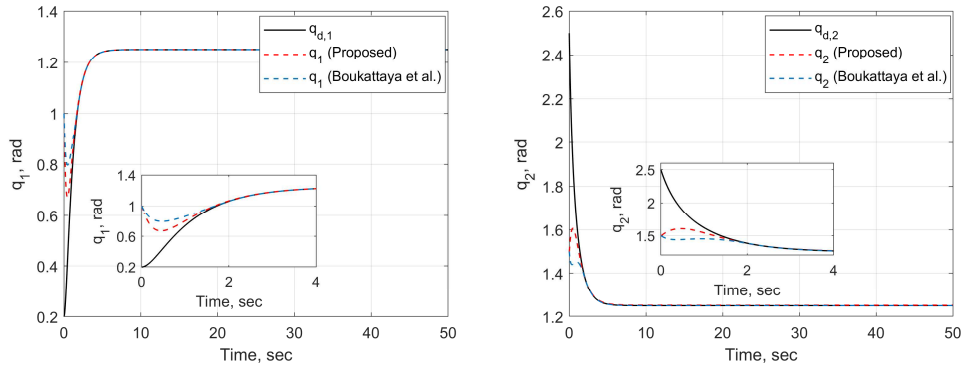


Fig. 9. Comparison of tracking responses under two types of controllers

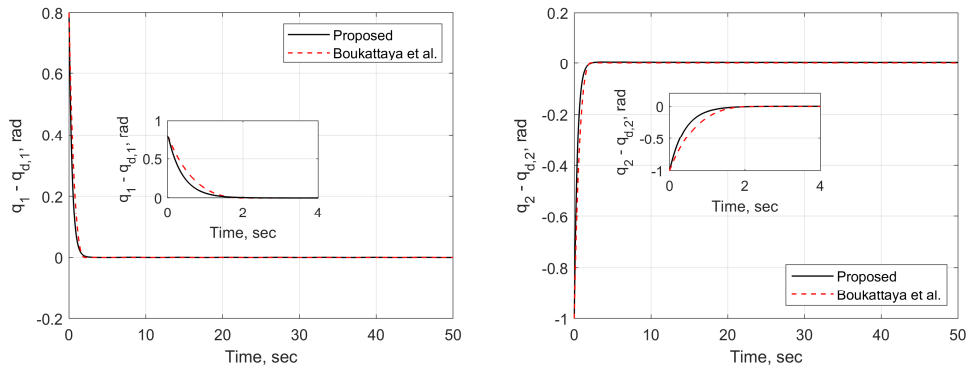


Fig. 10. Comparison of tracking errors under two types of controllers

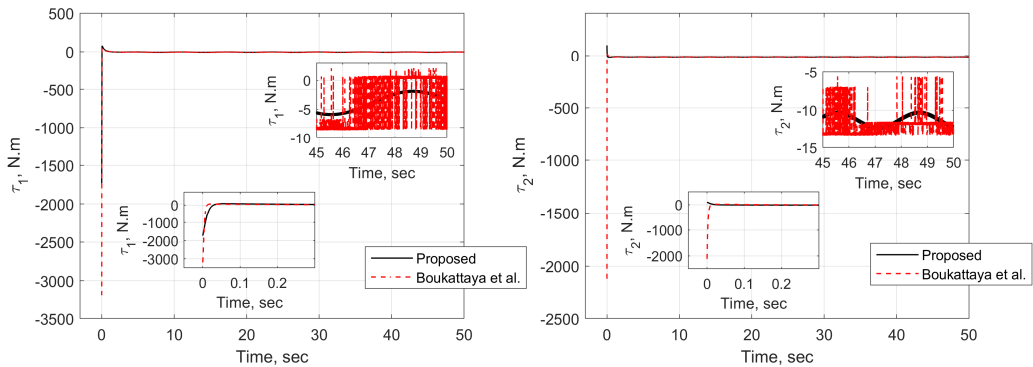


Fig. 11. Comparison of control input torques under two types of controllers

As mentioned earlier, the proposed control method requires the information of the nominal inertia matrix \mathbf{M}_0 to obtain the control input torques $\tau = \mathbf{M}_0 u$, where u is of PD form as described in eq. (20). However, it can be shown that even a poor estimate of \mathbf{M}_0 results in fairly good tracking performance. For example, assume that the nominal values of mass and inertia are poorly estimated as 30 % of their real values such that

$$\begin{aligned} \hat{m}_1 &= 0.3m_1 = 0.18 \text{ kg}, \quad \hat{m}_2 = 0.3m_2 = 0.54 \text{ kg}, \\ \hat{J}_1 &= 0.3J_1 = 1.8 \text{ kg} \cdot \text{m}^2, \quad \hat{J}_2 = 0.3J_2 = 1.8 \text{ kg} \cdot \text{m}^2. \end{aligned} \tag{60}$$

The poorly estimated values of eq. (60) were used both in the proposed APDC and the ANFTSMC proposed in [15] to control the robot manipulator while all the other parameters remained the same. Figures 12 and 13 show the tracking errors and the control input torques, respectively, obtained by applying both methods where the same control parameters as in eqs. (49) and (57) were used. The proposed method again yields faster convergence to the desired signals and the steady-state errors are much smaller than when the ANFTSMC with the poor estimates is applied. Also, the initial magnitude of the control torques is smaller, which is expected from eq. (52) with smaller \hat{m}_1 , \hat{m}_2 , \hat{J}_1 , and \hat{J}_2 . The chattering-like signals obtained from the APDC in Fig. 13 are caused by the attempt to mitigate the high-frequency disturbances given in eq. (47). The performance indices are listed in Table 2. Overall, the proposed APDC guarantees smaller tracking errors with similar control effort and requires less computational cost than the nonlinear ANFTSMC. Comparing with Table 1, one can see that the proposed method is not sensitive to the variation of the nominal values while the performance of the ANFTSMC is deteriorated if the nominal values are poorly selected, which is



mainly due to the fact that the equivalent control τ_{eq} in eq. (53) comprises the nominal matrices \mathbf{M}_0 , \mathbf{C}_0 , and \mathbf{G}_0 . Hence, one can conclude that even with a poor estimate of the nominal values for the mass and inertia of the joints, the APDC still exhibits a good convergence rate, small tracking errors, and strong robustness.

Finally, the effects of the control parameters of the proposed control scheme are investigated. In the simulations, each of the following parameters is considered to explore its effects on the tracking errors and control torques: (i) ζ and ω_n , (ii) δ , (iii) η , and (iv) K_0 .

4.1 Effect of ζ and ω_n

When the initial tracking errors are nonzero, ζ and ω_n determine how fast the errors would decay and be stabilized around zero. In many cases ζ can be set as unity (critical damping) for the fastest decay with no overshoot or undershoot. They also affect the steady-state errors as indicated by Theorem because the ultimate error bound is calculated as $\|e\|_{\infty} \leq 2\zeta\delta / \omega_n$. In the simulations, three cases were considered; the value of ζ is set as unity for all cases and ω_n is selected as 1, 5, and 10 for each case. The tracking errors and the control torques for the three cases are provided in Figs. 14 and 15, respectively, and the performance indices are given in Table 3. It is observed that as ω_n increases, the initial error decays more quickly, the steady-state error gets smaller, but the required control torque becomes higher. Also, it is interesting to see that the IAEs are approximately inversely proportional to ω_n . For example, the IAEs for both joints with $\zeta = 1$, $\omega_n = 5$ are approximately twice the IAEs with $\zeta = 1$, $\omega_n = 10$.

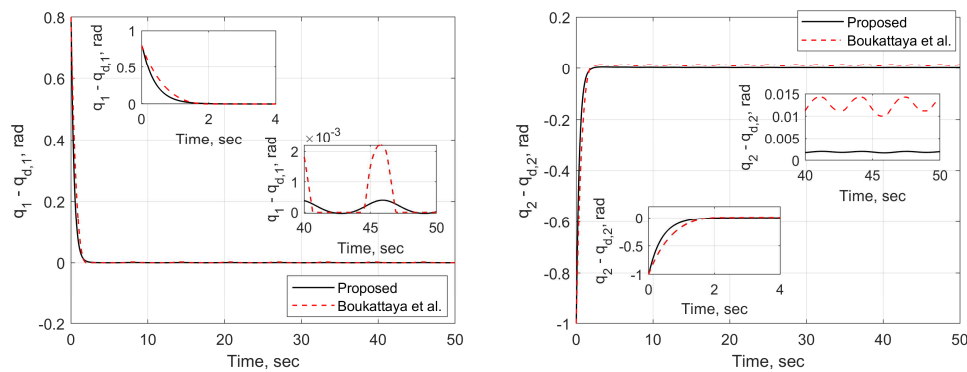


Fig. 12. Comparison of tracking errors under two types of controllers with poor estimates for nominal values

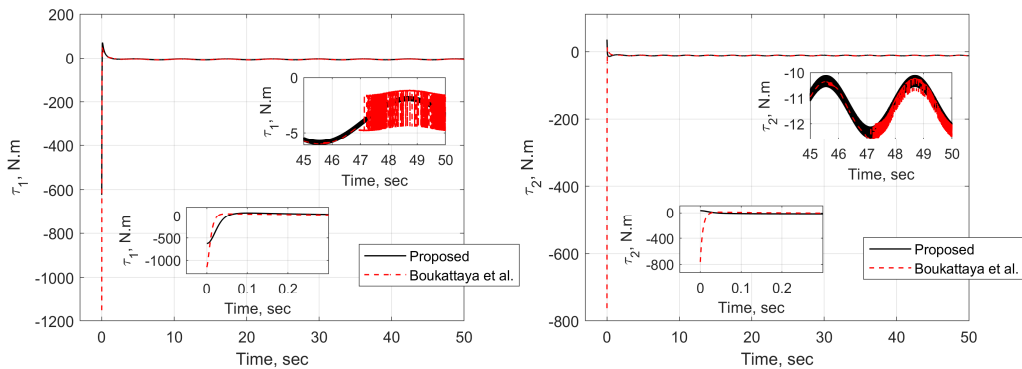


Fig. 13. Comparison of control input torques under two types of controllers with poor estimates for nominal values

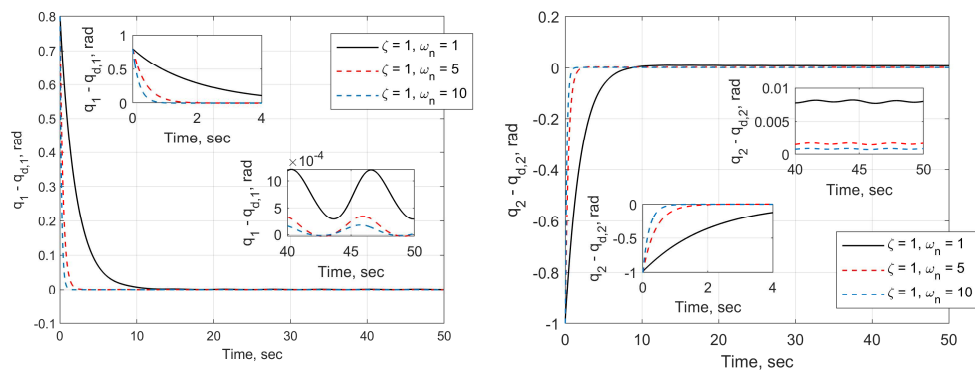


Fig. 14. Comparison of tracking errors when $\zeta = 1$ and $\omega_n = 1, 5, 10$



Table 2. Comparison of the performance indices with poor estimates for nominal values

Controller	IAE (rad-s)		IACT (m-N-s)		CT (s)
	Joint 1	Joint 2	Joint 1	Joint 2	
Proposed Controller	0.3292	0.4929	224.4	564.7	1.8529
Boukattaya et al. Controller [15]	0.4442	1.1370	218.7	568.9	7.1346

Table 3. Comparison of the performance indices when $\zeta = 1$ and $\omega_n = 1, 5, 10$

Parameters	IAE (rad-s)		IACT (m-N-s)	
	Joint 1	Joint 2	Joint 1	Joint 2
$\zeta = 1, \omega_n = 1$	1.6470	2.1991	220.1	570.9
$\zeta = 1, \omega_n = 5$	0.3256	0.4776	227.0	564.7
$\zeta = 1, \omega_n = 10$	0.1640	0.2411	258.4	591.9

Table 4. Comparison of the performance indices when $\delta = 0.001, 0.005, 0.01$

Parameters	IAE (rad-s)		IACT (m-N-s)	
	Joint 1	Joint 2	Joint 1	Joint 2
$\delta = 0.001$	0.3219	0.4148	229.2	564.3
$\delta = 0.005$	0.3256	0.4776	227.0	564.7
$\delta = 0.01$	0.3306	0.5583	225.8	565.4

4.2 Effect of δ

In this simulation, different numbers for δ ($\delta = 0.001, 0.005, 0.01$) are used to examine its effect on tracking performance and control cost while all the other parameters remain the same as in eq. (49). It will affect the steady-state response because the ultimate error is bounded by $\|e\|_{\infty} \leq 2\zeta\delta / \omega_n$. Figures 16 and 17 show the tracking errors and the computed input torques for the three different δ values. As expected, the transient response is scarcely affected by the change of the δ values, however, the steady-state response highly depends on the selection of δ . In general, as the value of δ increases, the steady-state error also increases as expected. Also, a larger δ results in a smaller initial magnitude of the control torques. Table 4 compares the performance indices for the three cases in terms of the IAEs and the IACTs. As the value of δ increases, the corresponding IAE also increases, but not very significantly when compared with Table 3. This can be explained by the fact that the transient response remains very similar for all cases and the steady-state error mainly contributes to the differences in the IAEs. The control cost in terms of the IACTs is not much affected by the variation of the δ values.

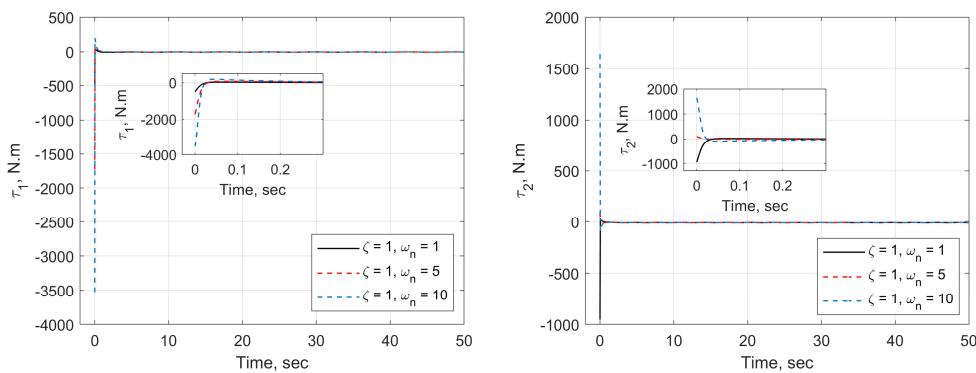


Fig. 15. Comparison of control input torques when $\zeta = 1$ and $\omega_n = 1, 5, 10$

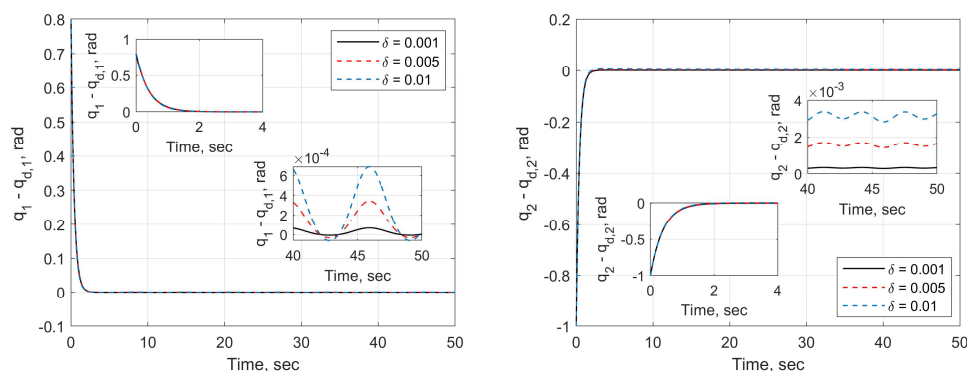


Fig. 16. Comparison of tracking errors when $\delta = 0.001, 0.005, 0.01$



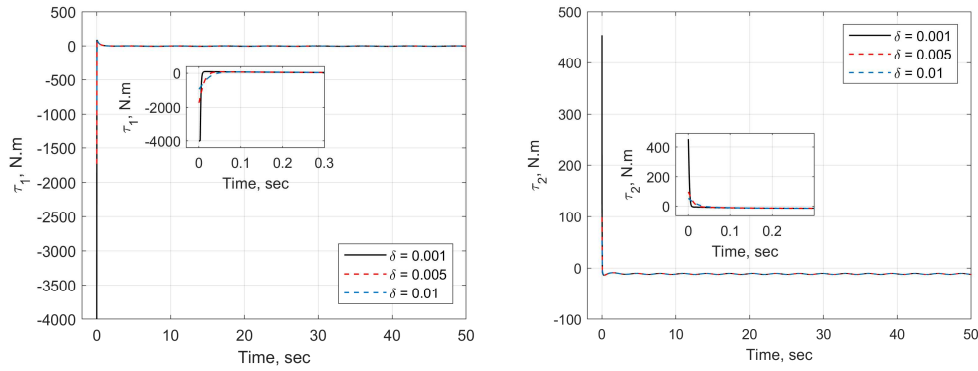


Fig. 17. Comparison of control input torques when $\delta = 0.001, 0.005, 0.01$

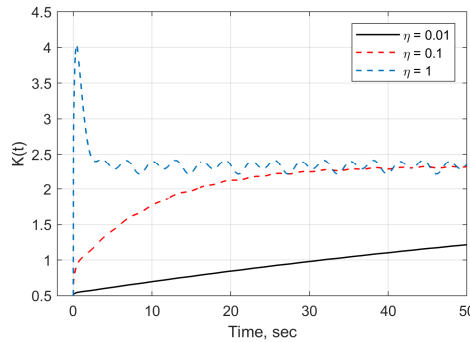


Fig. 18. time history of gain $K(t)$ when $\eta = 0.01, 0.1, 1$

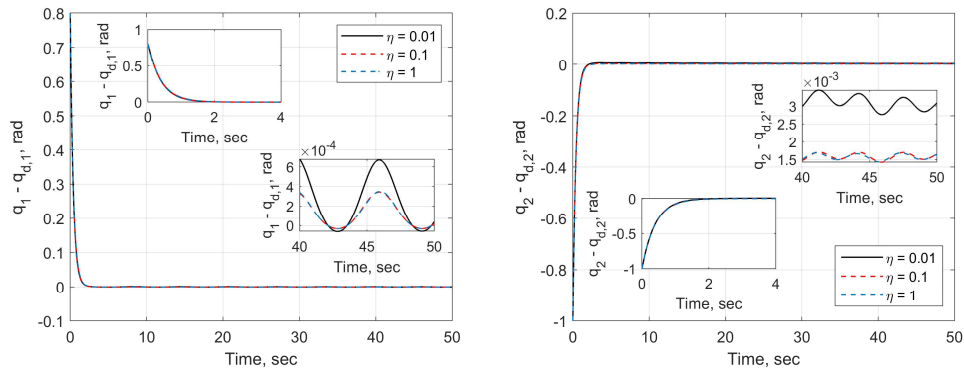


Fig. 19. Comparison of tracking errors when $\eta = 0.01, 0.1, 1$

4.3 Effect of η

From eq. (17) one can notice that η determines how fast the gain $K(t)$ changes. If η is selected too small, $K(t)$ cannot increase or decrease promptly when needed for error reduction or uncertainty suppression. If η is chosen too large, $K(t)$ may have a sudden rise, leading to a drastic change in the control torque from eq. (20), which is usually not desirable. Figure 18 shows the time history of $K(t)$ when η is selected as 0.01, 0.1, and 1. For the case $\eta = 0.01$, the rate of change of $K(t)$ is severely limited, and so the gain is insufficient to reduce the errors and to mitigate the uncertainty effects. If $\eta = 0.1$ is chosen, $K(t)$ smoothly increases to reduce the initial errors and finally converges to about 2.3 to stabilize the steady-state errors under the time-varying disturbances and model uncertainties. When $\eta = 1$, the gain drastically increases in the initial phase to diminish the initial errors and quickly converges to but oscillates (because of the high gain rate η) around 2.3 to mitigate the uncertainty and disturbance effects. Figures 19 and 20 present the tracking errors and the control torques. The transient response is not much influenced by the change of η , but a too small η (0.01) yields larger steady-state errors because $K(t)$ could not increase sufficiently quickly as seen from Fig. 18. Both $\eta = 0.1$ and $\eta = 1$ result in quite similar steady-state errors. From Fig. 20 when $\eta = 1$, the control torques drastically rise in wrong directions in the initial phase and so require a greater initial magnitude than the other two cases. Table 5 compares the performance indices for the three cases in terms of the IAEs and the IACTs. The IAEs have the greatest values for case $\eta = 0.01$ as expected because of the insufficient gain and the other two cases yield similar IAEs. Also, the control cost is not much affected by the selection of η .



Table 5. Comparison of the performance indices when $\eta = 0.01, 0.1, 1$

Parameters	IAE (rad·s)		IACT (m·N·s)	
	Joint 1	Joint 2	Joint 1	Joint 2
$\eta = 0.01$	0.3315	0.5794	227.6	565.7
$\eta = 0.1$	0.3256	0.4776	227.0	564.7
$\eta = 1$	0.3278	0.4712	229.1	564.8

Table 6. Comparison of the performance indices when $K_0 = 0.05, 0.5, 5$

Parameters	IAE (rad·s)		IACT (m·N·s)	
	Joint 1	Joint 2	Joint 1	Joint 2
$K_0 = 0.05$	0.3333	0.5024	221.5	564.6
$K_0 = 0.5$	0.3256	0.4776	227.0	564.7
$K_0 = 5$	0.3228	0.4342	229.4	564.4

4.4 Effect of K_0

Let us examine the effect of K_0 on tracking performance and control cost. Three different factors of K_0 (0.05, 0.5, 5) are used to control the manipulator and the initial gain $K(0)$ is set as the same as K_0 . All the other parameters remain the same as shown in eq. (49). Figure 21 presents the time history of $K(t)$ (left) and $K(t) - K_0$ (right). As proven earlier, $K(t)$ is always greater than or equal to K_0 and monotonically increasing with time in all cases. It is observed that a larger K_0 yields a greater $K(t)$, but the difference $K(t) - K_0$ is relatively small between each case. Also, the final value of $K(t) - K_0$ approximately converges to 1.8 for all cases. Figures 22 and 23 depict the tracking errors and the control torques, respectively. One can see that the transient responses are very similar but the steady-state error is smaller for a larger K_0 , which is expected from Fig. 21 where a larger K_0 yields a greater $K(t)$ to better suppress the error resulted from the external disturbances. However, the initial control magnitude is also huge for a large K_0 value as seen from Fig. 23. Table 6 compares the performance indices for the three cases in terms of the IAEs and the IACTs. The IAEs have the smallest values when $K_0 = 5$ because the corresponding gain $K(t)$ is the largest among three. Also, the control cost seems to increase as K_0 gets larger, but not significantly.

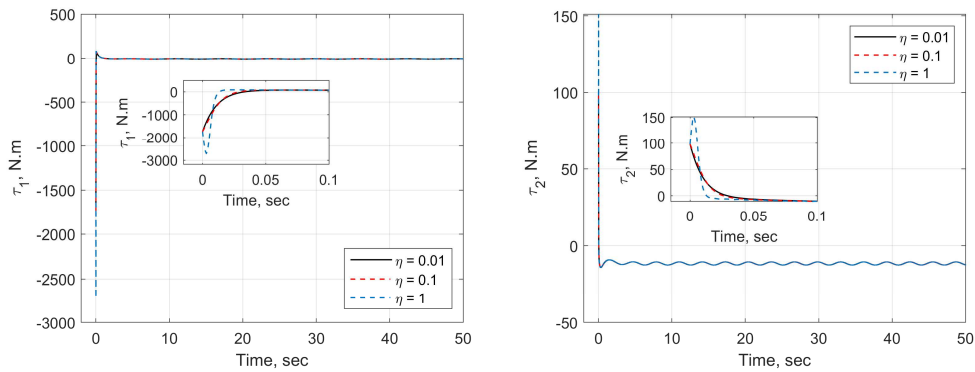


Fig. 20. Comparison of control input torques when $\eta = 0.01, 0.1, 1$

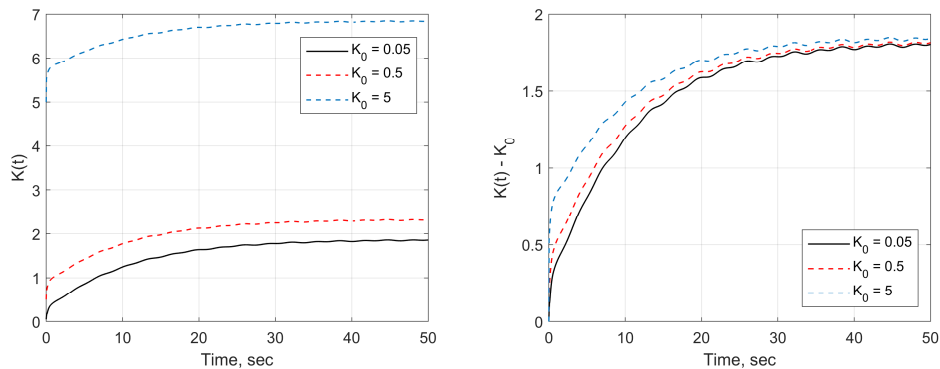


Fig. 21. Time history of $K(t)$ and $K(t) - K_0$ when $K_0 = 0.05, 0.5, 5$



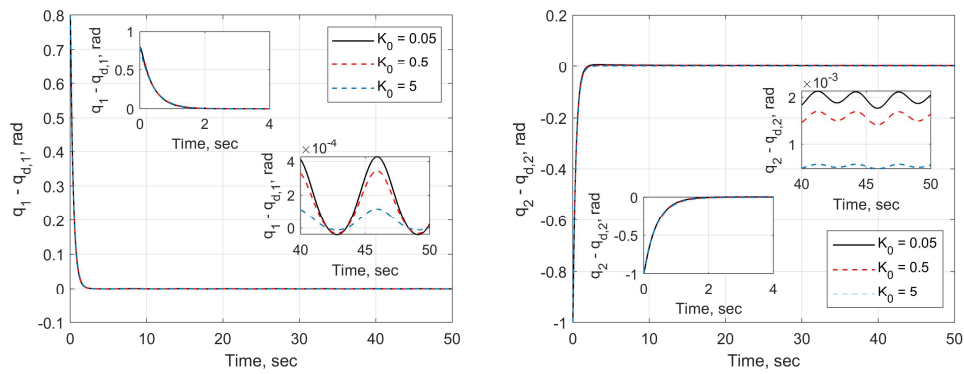


Fig. 22. Comparison of tracking errors when $K_0 = 0.05, 0.5, 5$

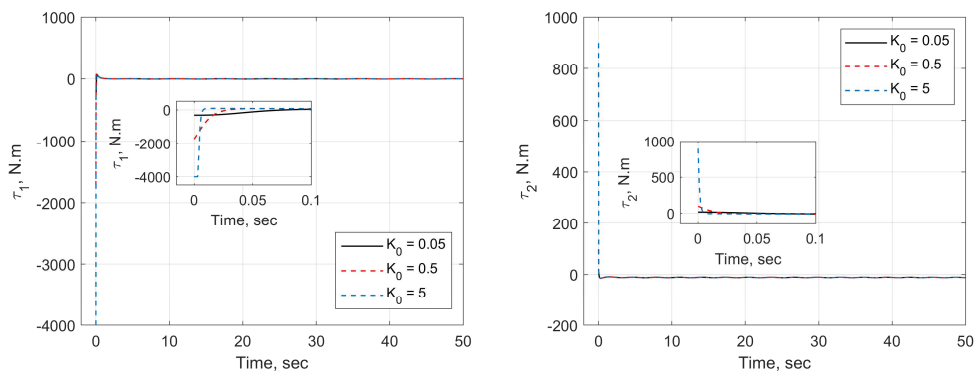


Fig. 23. Comparison of control input torques when $K_0 = 0.05, 0.5, 5$

5. Conclusion

In this paper, the trajectory tracking problem of robot manipulators in the presence of model uncertainties and external disturbances was investigated and a new adaptive PD control (APDC) method was proposed. This approach has the advantages of simple linear control and robust adaptive control without any a priori information about the bounds on the uncertainties or disturbances. The control acceleration is a feedback control law that only includes the tracking errors and their derivatives, and the corresponding control torque is obtained by multiplying the obtained control acceleration with the nominal inertia matrix. It was shown that even a poor estimate of the nominal inertia matrix leads to fairly good tracking performance, which shows little sensitivity to the selection of the nominal parameters. On the other hand, the existing sliding mode control approach with imprecise nominal values suffers from huge tracking errors. The computational simplicity and easy design of the proposed control strategy are another advantage. In the considered numerical example, the APDC performs better than the existing fast terminal nonsingular sliding mode control method in terms of faster convergence, better tracking performance, less computational cost, and no chattering. In addition, the effects of the various control parameters on tracking accuracy and control cost were investigated to provide a direction of how to select good parameters to achieve desired performance. Future work will include the experimental validation of the proposed APMC method using a real robotic system. Also, the optimization of control parameters to balance between the tracking error and the control effort will be conducted and a novel differentiator will be developed to design output feedback control without velocity measurements.

Conflict of Interest

The author declared no potential conflicts of interest with respect to the research, authorship, and publication of this article.

Funding

The author received no financial support for the research, authorship, and publication of this article.

References

- [1] Dixon, W.E., Zergeroglu, E., Dawson, D.M., Global Robust Output Feedback Tracking Control of Robot Manipulators, *Robotica*, 22(4), 2004, 351–357.
- [2] Purwar, S., Kar, I.N., Jha, A.N., Adaptive Output Feedback Tracking Control of Robot Manipulators Using Position Measurements Only, *Expert Systems with Applications*, 34(4), 2008, 2789–2798.
- [3] Shojaei, K., Shahri, A.M., Tarakameh, A., Adaptive Feedback Linearizing Control of Nonholonomic Wheeled Mobile Robots in Presence of Parametric and Nonparametric Uncertainties, *Robotics and Computer-Integrated Manufacturing*, 27(1), 2011, 194–204.
- [4] Hu, Q., Xu, L., Zhang, A., Adaptive Backstepping Trajectory Tracking Control of Robot Manipulator, *Journal of the Franklin Institute*, 349(3), 2012, 1087–1105.
- [5] Chen, N., Song, F., Li, G., Sun, X., Sheng, C., An Adaptive Sliding Mode Backstepping Control for the Mobile Manipulator with Nonholonomic Constraints, *Communications in Nonlinear Science and Numerical Simulation*, 18(10), 2013, 2885–2899.
- [6] Nikdel, N., Badamchizadeh, M.A., Azimirad, V., Nazari, M.A., Adaptive Backstepping Control for an n-Degree of Freedom Robotic Manipulator Based on Combined State Augmentation, *Robotics and Computer-Integrated Manufacturing*, 44, 2017, 129–143.



- [7] Chen, B.S., Chang, Y.C., Lee, T.C., Adaptive Control in Robotic Systems with H_∞ Tracking Performance, *Automatica*, 33(2), 1997, 227–234.
- [8] Sato, K., Mukai, H., Tsuruta, K., An Adaptive H_∞ Control for Robotic Manipulator with Compensation of Input Torque Uncertainty, 17th IFAC World Congress, Seoul, Korea, 2008.
- [9] Rigatos, G., Siano, P., Raffo, G., A Nonlinear H-infinity Control Method for Multi-DOF Robotic Manipulators, *Nonlinear Dynamics*, 88, 2017, 329–348.
- [10] Tang, Y., Arteaga, M.A., Adaptive Control of Robot Manipulators Based on Passivity, *IEEE Transactions on Automatic Control*, 39(9), 1994, 1871–1875.
- [11] Bouakrif, F., Boukhetala, D., Boudjema, F., Passivity-Based Controller-Observer for Robot Manipulators, 3rd International Conference on Information and Communication Technologies: From Theory to Applications, Damascus, Syria, 2008.
- [12] Zhang, Y., Li, S., Zou, J., Khan, A.H., A Passivity-Based Approach for Kinematic Control of Manipulators with Constraints, *IEEE Transactions on Industrial Informatics*, 16(5), 2020, 3029–3038.
- [13] Zhihong, M., O'Day, M., Yu, X., A Robust Adaptive Terminal Sliding Mode Control for Rigid Robotic Manipulators, *Journal of Intelligent and Robotic Systems*, 24, 1999, 23–41.
- [14] Jin, M., Lee, J., Chang, P.H., Choi, C., Practical Nonsingular Terminal Sliding-Mode Control of Robot Manipulators for High-Accuracy Tracking Control, *IEEE Transactions on Industrial Electronics*, 56(9), 2009, 3593–601.
- [15] Boukattaya, M., Mezghani, N., Damak, T., Adaptive Nonsingular Fast Terminal Sliding-Mode Control for the Tracking Problem of Uncertain Dynamical Systems, *ISA Transactions*, 77, 2018, 1–19.
- [16] Soltanpour, M.R., Zaare, S., Haghgoo, M., Moattari, M., Free-Chattering Fuzzy Sliding Mode Control of Robot Manipulators with Joints Flexibility in Presence of Matched and Mismatched Uncertainties in Model Dynamic and Actuators, *Journal of Intelligent & Robotic Systems*, 100, 2020, 47–69.
- [17] Udawadia, F.E., Wanichanon, T., A New Approach to the Tracking Control of Uncertain Nonlinear Multi-body Mechanical Systems, *Book of 'Nonlinear Approaches in Engineering Applications 2' (Edited by Jazar, R.N., Dai, L.)*, Springer, New York, 2014, 101–136.
- [18] Udawadia, F.E., Wanichanon, T., Control of Uncertain Nonlinear Multibody Mechanical Systems, *Journal of Applied Mechanics*, 81(4), 2014, 041020-1 – 041020-11.
- [19] Wanichanon, T., Cho, H., Udawadia, F.E., Satellite Formation-Keeping Using the Fundamental Equation in the Presence of Uncertainties in the System, *AIAA SPACE 2011 Conference & Exposition*, Long Beach, USA, 2011.
- [20] Cho, H., Wanichanon, T., Udawadia, F.E., Continuous Sliding Mode Controllers for Multi-Input Multi-Output Systems, *Nonlinear Dynamics*, 2018, 2727–2747.
- [21] Cho, H., Kerschen, G., Oliveira, T.R., Adaptive smooth control for nonlinear uncertain systems, *Nonlinear Dynamics*, 99, 2020, 2819–2833.
- [22] Kawamura, S., Miyazaki, F., Arimoto, S., Is a Local Linear PD Feedback Control Law Effective for Trajectory Tracking of Robot Motion?, 1988 *IEEE International Conference on Robotics and Automation*, Philadelphia, USA, 1988.
- [23] Sage, H.G., De Mathelin, M.F., Ostertag, E., Robust Control of Robot Manipulators: A Survey, *International Journal of Control*, 72(16), 1999, 1498–1522.
- [24] Craig, J.J., *Introduction to Robotics: Mechanics and Control*, Prentice Hall, Boston, 2004.
- [25] Spong, M.W., Hutchinson, S., Vidyasagar, M., *Robot Modeling and Control*, volume 3, Wiley, New York, 2006.
- [26] Kelly, R., A Tuning Procedure for Stable PID Control of Robot Manipulators, *Robotica*, 13, 1995, 141–148.
- [27] Cervantes, I., Alvarez-Ramirez, J., On the PID Tracking Control of Robot Manipulators, *Systems & Control Letters*, 42(1), 2001, 37–46.
- [28] Arimoto, S., Fundamental Problems of Robot Control: Part I, Innovations in the Realm of Robot Servo-Loops, *Robotica*, 13(1), 1995, 19–27.
- [29] Kelly, R., Global Positioning of Robot Manipulators via PD Control plus a Class of Nonlinear Integral Actions, *IEEE Transactions on Automatic Control*, 43(7), 1998, 934–938.
- [30] Jafarov, E.M., Parlakci, M.N.A., I Stefanopoulos, Y., A New Variable Structure PID-Controller Design for Robot Manipulators, *IEEE Transactions on Control Systems Technology*, 13(1), 2005, 122–130.
- [31] Nunes, E.V.L., Hsu, L., Global Tracking for Robot Manipulators Using a Simple Causal PD Controller plus Feedforward, *Robotica*, 28(1), 2010, 23–34.
- [32] Gorez, R., Globally Stable PID-like Control of Mechanical Systems, *Systems & Control Letters*, 38(1), 1999, 61–72.
- [33] Su, Y., Müller, P.C., Zheng, C., Global Asymptotic Saturated PID Control for Robot Manipulators, *IEEE Transactions on Control Systems Technology*, 18(6), 2010, 1280–1288.
- [34] Mendoza, M., Zavala-Rio, A., Santibanez, V., Reyes, F., Output-Feedback Proportional-Integral-Derivative-type Control with Simple Tuning for the Global Regulation of Robot Manipulators with Input Constraints, *IET Control Theory & Applications*, 9(14), 2015, 2097–2106.
- [35] Tomei, P., Adaptive PD Controller for Robot Manipulators, *IEEE Transactions on Robotics and Automation*, 7(4), 1991, 565–570.
- [36] Burkan, R., Design of an Adaptive Control Law Using Trigonometric Functions for Robot Manipulators, *Robotica*, 23(1), 2005, 93–99.
- [37] Xu, J., Qiao, L., Robust Adaptive PID Control of Robot Manipulator with Bounded Disturbances, *Mathematical Problems in Engineering*, 2013, 2013, 1–13.
- [38] Nohooji, H.R., Constrained Neural Adaptive PID Control for Robot Manipulators, *Journal of the Franklin Institute*, 357(7), 2020, 3907–3923.
- [39] Gronwall, T.H., Note on the Derivatives with Respect to a Parameter of the Solutions of a System of Differential Equations, *Annals of Mathematics, Second Series*, 20(4), 1919, 292–296.
- [40] Boyd, S., Vandenberghe, L., *Convex Optimization*, Cambridge University Press, Cambridge, 2004.
- [41] Khalil, H.K., *Nonlinear Control*, Pearson, Essex, 2015.

ORCID iD

Hancheol Cho  <https://orcid.org/0000-0002-3245-0757>



© 2020 by the authors. Licensee SCU, Ahvaz, Iran. This article is an open access article distributed under the terms and conditions of the Creative Commons Attribution-NonCommercial 4.0 International (CC BY-NC 4.0 license) (<http://creativecommons.org/licenses/by-nc/4.0/>).

How to cite this article: Cho H. On Robust Adaptive PD Control of Robot Manipulators, *J. Appl. Comput. Mech.*, 6(SI), 2020, 1450–1466. <https://doi.org/10.22055/JACM.2020.35658.2707>

